Biochimica et Biophysica Acta 813 (1985) 41–50
Elsevier

BBA 72454

Temperature effects on osmotic fragility, and the erythrocyte membrane

Gary V. Richieri and Howard C. Mel

Department of Biophysics and Medical Physics, University of California, Berkeley, CA 94720 (U.S.A.)

(Received September 3rd, 1984)

Key words: Osmotic fragility; Temperature dependence; Cell volume; Erythrocyte membrane

Results are reported on the temperature-dependence of intact-cell surface area, isotonic volume, hemolytic volume, and ghost steady-state surface area and volume, using several techniques of resistive pulse spectroscopy. Temperature was found not to alter the intact cell surface area permanently: the area remains constant at 130 ± 1 μm^2, at temperatures ranging from 0 to 40°C. Temperature does alter the steady-state volume of the cells, with a colder temperature inducing swelling by about 0.29 μm^3/deg. C. Such a temperature-induced volume change is sufficient to explain only approximately half of the fragility differences which result from temperature changes. The remainder was found to result from higher temperatures enabling a substantial transient increase in surface area of intact cells (up to at least 14% at 40°C), with a corresponding increase in the cell's hemolytic volume (up to 21%). The hemolytic volume apparently increases linearly with temperature, since steady-state ghost volumes are found to increase lineary with the temperature at which the ghosts were produced. In the steady state (at high temperature), the membranes of electrically-impermeable resealed ghosts can remain extended by more than 10%, compared with membranes of the corresponding unhemolyzed, intact red cells.

Introduction

It has long been known that temperature is a major factor in red cell fragility, resulting in resistance to hemolysis that increases with increasing temperature [1–3]. A number of different proposals have been advanced to explain this finding.

(1) Proposal one is that the isotonic volume of the cell is, itself, temperature dependent, with high temperatures causing a decrease in volume at constant surface area [2,4]. This response would also increase the surface-to-volume ratio, and decrease the osmotic fragility. However, neither Murphy (by microhematocrit [5]), nor Seeman et al. (by Coulter-type sizing [3]) were able to detect such an effect experimentally.

(2) Proposal two is that the surface area, alone, (hence the surface-to-volume ratio), increases with temperature [5,6]; this would require, for the higher temperatures, a greater volume increase and hence a lower osmolality to cause the cells to swell to their now larger spherical volume. However, early work by others (which was only able to determine steady-state volumes) showed the spherical volumes to be independent of temperature [2,3].

(3) Proposal three invokes a temperature-dependent leakage of potassium, occurring at the cell's critical volume stage (with attendant loss of water), to reduce the osmotic fragility. Ponder and Robinson [7], and Davson [8], reported such potassium leakage (of up to 8% of the cell's potassium content) at room temperature, and Seeman et al. [3] advanced the theory that this leak was temperature dependent: more leak at higher temperature. How-

0005-2736/85/$03.30

ever, Livne and Raz [9] reported finding no difference in leak, over a temperature range of 5 to 37°C.

Both proposals two and three are clearly membrane-dominated phenomena.

(4) A forth proposal of this same character that appears not to have been considered, as yet, would be an increase in membrane mechanical strength in response to increasing temperature, accompanied by little, if any, surface or volume change.

(5) A fifth proposal is that fragility changes have their origins in a cytoplasmic response (such as a change in the osmotic coefficient of hemoglobin). Aloni et al. [10] performed temperature-fragility experiments on cells containing various amounts of hemoglobin, and found that the same temperature dependence was present irrespective of the hemoglobin concentration. These authors thus concluded that the temperature has its effect on the membrane of the cell rather than on this (the cell's principal) cytoplasmic component.

The present study uses resistive pulse spectroscopy to investigate osmotic fragility and the interrelated properties of volume, form, and surface area for intact cells, hemolyzing cells, and ghosts. New results are reported on the temperature-dependence of surface area, isotonic volume, and hemolytic volume. From these results we are able to arrive at a unifying view of these interrelated factors insofar as they effect osmotic fragility. One noteworthy conclusion from this work is that under certain conditions the red cell membrane can sustain an astonishing degree of stretch without hemolysis.

Materials and Methods

Sample preparation. A stock suspension of red blood cells consists of two drops of blood from a normal adult finger prick, suspended in 10 ml of 'isotonic' phosphate-buffered saline (Dulbecco's PBS (pH 7.4), 300 mosmolal [11]). To avoid transients in osmotic fragility and volume properties, the cells are allowed to equilibrate with the solution for about one hour before tests are initiated. For the actual measurements, a secondary dilution is then made by transferring 0.2 ml of the stock to 10 ml of the test solution, yielding a final cell concentration on the order of 10^5 cells/ml. Variations in osmolality of the test solution are obtained by adding either NaCl or deionized water to the 300 mosmolal medium. Osmolality measurements are made with a Fiske model G-62 freezing point osmometer (Fiske Associates, Inc., Uxbridge, MA). For the studies that involve temperature as an independent variable both the stock and test solutions are at the same temperature.

Instrumentation. The analytical method of resistive pulse spectroscopy has been described previously [12]. Briefly, it is an outgrowth and extension of electronic cell sizing ('Coulter counting') that permits determination of several cell biophysical properties other than just number and volume, including fragility, deformability, form, and surface area (Refs. 12 and 13; Richieri, G.V., Akeson, S.P. and Mel, H.C., unpublished data). This and other information is inherent in, and can be deduced from, spectra of resistive pulses generated by the rheological and electrical interaction of cells flowing through a current-limiting orifice. The orifice we use is cylindrical, 48×48 μm (diameter by length), obtained from Particle Data (Elmhurst, IL). At least four measurements are made for each data point, with the standard deviation being less than 1%.

Unlike traditional cell fragility-measuring methods, which assay released hemoglobin, in resistive pulse spectroscopy it is the percentage of ghosts which is measured [12–14]. To accomplish this most accurately the cell populations are sized with a high electric field which renders the cell-membrane electrically transparent. The ghosts appear sufficiently smaller in size than non-ghosts, to be separately countable, even if the two are of equal true volume.

Theoretical analysis. The complete mathematical determination of volume and form from a resistive-pulse-produced spectrum will be fully developed in a future publication, but it is summarized below. In traditional electronic cell sizing, a priori assumptions on cell shape are required as correction factors to the experimentally measured volumes. However, according to this new application of resistive pulse spectroscopy, it is possible to deduce both volume and shape information, and surface area, simultaneously. This is accomplished, in part, (a) by sizing at a low fluid-flow rate (less than 1.1 m/s) to eliminate deformational shape changes; (b) by measuring critically swollen as well as isotonic volumes; and (c) by utilizing electric fields within the orifice that are kept below the membrane dielectric breakdown potential (i.e. less than 1 kV/cm) [15].

If the surface area of a cell is constant, and the cell shape is restricted to a particular form class (for this paper we will use the oblate ellipsoidal shape), any volume change results in a specific change in shape factor. The relationship between the measured volume, true volume, and shape factor (f_E) is [16]:

$$\mathrm{Vol(meas)} = \mathrm{Vol(true)} \cdot f_E \tag{1}$$

where f_E equals 1.5 for a sphere.

The unifying relationships between these three factors depend upon the independent variables: a (major semiaxis), and b (minor semiaxis), (and on the ratio a/b). The equations for oblate ellipsoids of revolution are as follows (Richieri, G.V., Akeson, S.P. and Mel, H.C. (1984)):

$$\mathrm{Vol(true)} = \tfrac{4}{3}\pi a^2 b \tag{2}$$

$$\text{Surface area (S.A.)} = 2\pi a^2 + \pi \frac{b^2}{\epsilon} \ln\left(\frac{1+\epsilon}{1-\epsilon}\right) \tag{3}$$

where

$$\epsilon = \frac{(a^2-b^2)^{1/2}}{a};$$

$$f_E = 2/(2 - a^2 b L_b) \tag{4}$$

where

$$L_b = \frac{b}{a^2(b^2-a^2)} - \frac{1}{(a^2-b^2)^{3/2}} \tan^{-1}\left(\frac{b^2}{a^2-b^2}\right)^{1/2} + \frac{\pi}{2(a^2-b^2)^{3/2}}$$

$$\mathrm{Vol(true\text{-}max)} = (\mathrm{S.A.})^{3/2}/6\pi^{1/2} \tag{5}$$

$$\mathrm{Vol(meas\text{-}max)} = \mathrm{Vol(true\text{-}max)} \cdot 1.5 \tag{6}$$

Eqn. 1 divided by Eqn. 6 yields:

$$\frac{\mathrm{Vol(meas)}}{\mathrm{Vol(meas\text{-}max)}} = \frac{\mathrm{Vol(true)}}{\mathrm{Vol(true\text{-}max)}} \cdot \frac{f_E}{1.5} \tag{7}$$

From these seven equations two particularly useful relationships can be derived by proceeding as follows: (a) using Eqns. 2–5, tabulate the magnitudes of the factors in Eqn. 7 for many different a/b ratios; (b) plot the two relationships: f_E versus Vol(true)/Vol(true-max), and Vol(meas)/Vol(meas-max) versus Vol(true)/Vol(true-max); and (c) by computer, obtain the best fourth-order polynomial equations fitting the respective curves. Proceeding in this way, we arrive at the following two equations:

$$\frac{\mathrm{Vol(true)}}{\mathrm{Vol(true\text{-}max)}} = -2.979\,(f_E) + 15.206\,(f_E^2) - 10.576\,(f_E^3) + 2.120\,(f_E^4) - 3.787 \tag{8}$$

(correlation coefficient for fit of data: $r = 0.9988$); and

$$\frac{\mathrm{Vol(true)}}{\mathrm{Vol(true\text{-}max)}} = 1.544\,(X) - 0.854\,(X^2) + 0.846\,(X^3) - 0.531\,(X^4) - 0.0014 \tag{9}$$

where X is Vol(meas)/Vol(meas-max) and $r = 0.9999$.

Results

Temperature dependence of osmotic hemolysis

Human red blood cells, stored at various temperatures, were exposed to different low-osmolal-

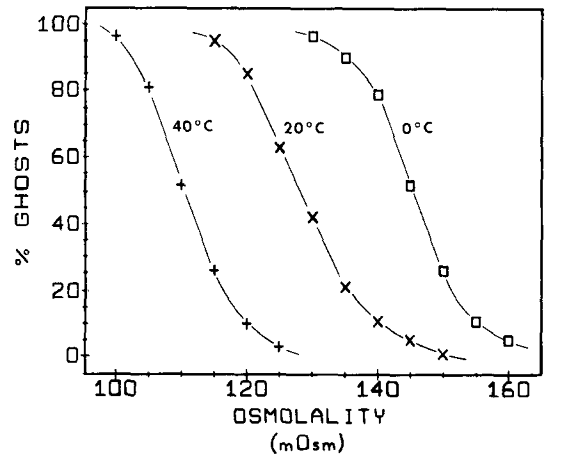

Fig. 1. Temperature dependence of osmotic fragility in diluted solutions of phosphate-buffered saline. The red cell concentration is approx. $2 \cdot 10^5$ cells/ml. (+, 40°C; ×, 20°C; and □, 0°C).

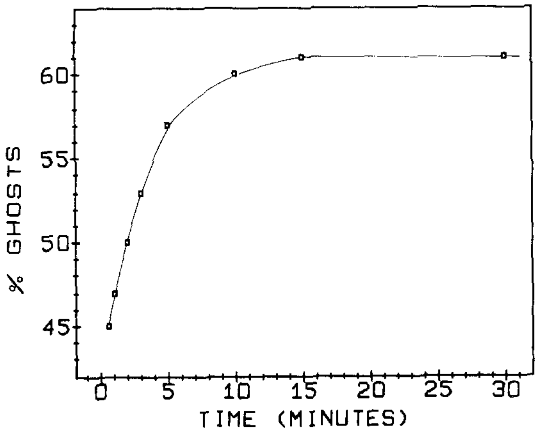

Fig. 2. Kinetics of red cell ghost formation demonstrated at 20°C, in a 125 mosmolal solution containing 0.42 mM calcium. (The extent to which hemolysis kinetics depend on Ca^{2+} concentration is given elsewhere (Richieri, G.V. (1984) Responses of red blood cell-membrane systems: Temperature and calcium effects on volume, deformability, and osmotic fragility. Ph.D. Thesis, University of California, Berkeley, Department of Biophysics and Medical Physics)).

ity solutions, and the percentages of ghosts measured. The results are given in Fig. 1. The values shown are from the steady states, after the cells have been in the hypotonic medium for at least 15 min (see Fig. 2). These are the basic data for which the five Proposals were advanced in the Introduction, by way of explanation.

Volume, surface area, and form of intact cells and ghosts

The true volumes, surface areas, and form factors of the intact cells in isotonic medium were determined from the measured volumes by means of the Theoretical Analysis-sizing protocol given in Materials and Methods. The experimental data are analyzed according to three alternative models of cell behavior in such a way as to permit decision on the 'best fit' set of parameters. The results of the three sets of calculations are tabulated in Table I, columns 3 and 4, 5 and 6, and 7, respectively, along with the measured or apparent volumes given in column 2.

The first of these models, Proposal 1 of the Introduction, considers the cells as oblate ellipsoids of revolution, and assumes that the surface area remains at a constant 130 μm^2 at all temperatures. The maximum spherical volume, thus, also remains constant, at 140 μm^3, but otherwise the volume may change. The values of volume and shape factor are determined by use of Eqns. 8 and 9 as follows: first the experimental measurements are reduced to a set of dimensionless ratios, (X), by dividing each measured size by the maximum size, both expressed in channel numbers. The maximum size for a 140 μm^3 spherical red cell is 55.3 channels. Substituting these X values in Eqn. 9, yields the corresponding values for the ratios Vol(true)/Vol(true-max). From these ratios and

TABLE I

THE ISOTONIC VARIATION IN APPARENT SIZE, INDUCED BY TEMPERATURE CHANGE, ACCORDING TO THREE DIFFERENT MODELS

Temp. (°C)	Apparent size (channels)	Model 1 (Surface area = 130 μm^2)		Model 2 (Volume = 88 μm^3)		Model 3 (Vol = 88 μm^3, S.A. = 130 μm^2)
		Vol ($\pm$ μm^3)	f_E ($\pm$0.006)	S.A. ($\pm$2 μm^2)	f_E ($\pm$0.006)	f_E ($\pm$0.006)
0	30.4	95.2	1.209	105	1.308	1.308
5	29.8	93.6	1.205	108	1.282	1.282
10	29.3	92.2	1.200	112	1.257	1.257
15	28.7	90.8	1.197	117	1.235	1.235
20	28.2	89.2	1.191	124	1.207	1.207
25	27.5	87.5	1.188	133	1.181	1.181
30	26.9	85.8	1.182	147	1.152	1.152
40	25.8	83.5	1.178	169	1.118	1.118

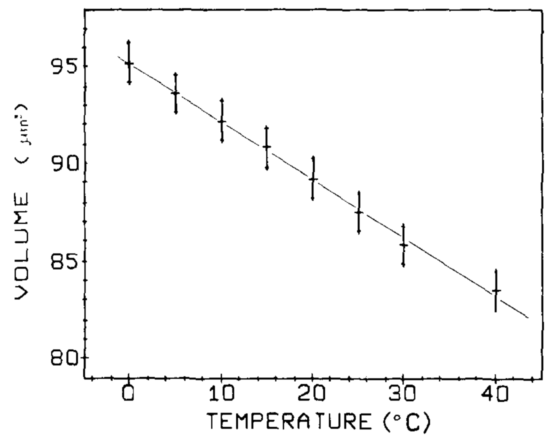

Fig. 3. Calculated 'true' volume (slow flow and oblate approximation) as a function of temperature for cells at 300 mosmolal assuming constancy of surface area (model one).

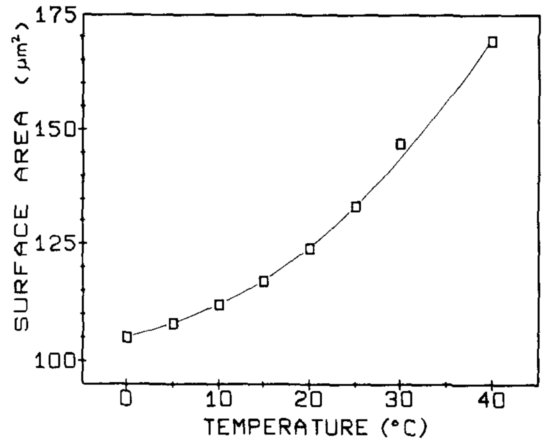

Fig. 4. Calculated surface area as a function of temperature for cells at 300 mosmolal assuming constancy of volume (model two).

Eqn. 8, we calculate the set of corresponding f_E values, column 4, Table I, and then (from Vol(true-max) = 140 μm^3) the set of Vol(true) values, column 3, Table I.

In Fig. 3 these volumes are plotted as a function of temperature. The volume is seen to decrease linearly with temperature, from 95.2 μm^3 at 0°C to 83.5 μm^3 at 40°C, according to the assumptions of this constant-surface model.

The second model, Proposal 2, also assumes that the shape remains as an oblate ellipsoid, but that the true, isotonic volume remains constant (taken as 88 μm^3), while the surface area changes, as necessary, to accommodate the data. The respective values of surface area and shape factor are calculated by noting that the product of the true volume and shape factor must be identical for any model, namely equal to the measured volume (Eqn. 1). Thus:

$$\frac{[\text{Vol(true)} \times \text{Shape factor}]_{\text{model 1}}}{[\text{Vol(true)} = 88\ \mu m^3]_{\text{model 2}}} = [\text{Shape factor}]_{\text{model 2}} \quad (10)$$

From Eqn. 10 and the data of Table I, columns 3 and 4, values for f_E are calculated, and tabulated in column 6 of Table I. Using these f_E values in Eqn. 8, allows calculation of the ratios Vol(true)/Vol(true-max) (model 2). Applying Vol(true) (model 2) = 88 μm^3 to these ratios, we calculate the set of Vol(true-max) values; then from Eqn. 5, the variable surface areas consistent with the model are calculated, and tabulated in column 5 of Table I.

In Fig. 4 we plot the results for this model, the surface area as a function of temperature. As seen, this model requires an increasing enlargement of the surface area with temperature, overall a 60% increase, from 0°C to 40°C.

The third model, though not one of the five initial proposals, is included as an alternative ex-

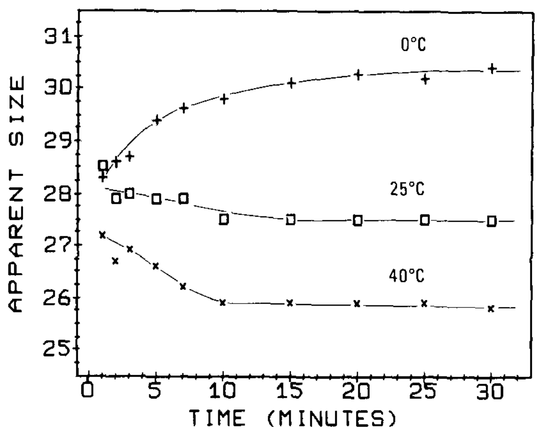

Fig. 5. Kinetics of apparent-size changes for cells stored for various times in primary dilution (isotonic medium) at different temperatures. Aliquots were subsequently removed for secondary dilution in isotonic medium at the same temperature as the primary dilution, for immediate measurement. (×, 40°; □, 25°; and +, 0°C).

planation for the differences in measured size. It assumes that the entire differences can be explained solely by an altered shape factor. The f_E values necessary to reconcile the data in this way are calculated according to Eqn. 10 and tabulated in Table I, column 7. (Note that this assumption necessarily violates the oblate-shape assumption, and in fact would require large distortions in shape-folding or tucking-in of membrane.)

In order to eliminate transients, the sizing experiments were all performed after the cells had been at their respective temperatures for at least one hour. The complete apparent-size kinetics are depicted in Fig. 5. As seen, the cells require times ranging from 10 to 30 min in their primary stock suspension to reach their steady-state condition.

Comparison of models 1 and 2. A direct experimental means of distinguishing between the contradictory models (alterations in volume as compared to surface area) is to size the cells after they have been swollen to spheres. If they all have the same spherical size then the surface area has necessarily remained constant; if not, then the surface area is temperature-dependent.

Cells, at different temperatures, were placed in media of appropriate osmolality so as to yield a small percentage (less than 10%) of ghosts. (Fig. 1 was used to select the osmolalities.) The percentages of ghosts were kept low in this manner in order to minimize interference with the intact-spherical-cell size spectra. The presence of some ghosts in the mixture insured that the model size of intact cells would be characteristic of the cells swollen to their spherical state. In this condition we were able to use the single shape factor of 1.5 to determine the true volume (Eqn. 1), independent of either model.

The volumes of the spherical intact cells are shown in Fig. 6 (squares, bottom line); these volumes are independent of temperature, they are all approx. 140 μm^3, as reported previously [2,3]. It is from this 140 μm^3 value that we calculate the 130 μm^2 constant surface area value.

Ghost volumes. Also included in Fig. 6 are the ghosts volumes (circles). To measure these, the cells were placed in osmolalities sufficiently low to cause greater than 95% ghosts in the population, and thus to eliminate distortion in the size spectra arising from non-ghosts. Again, Fig. 1 was used to

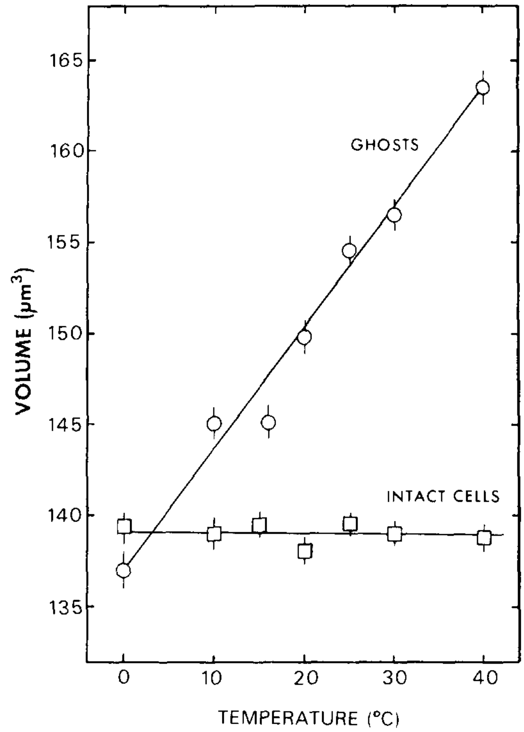

Fig. 6. The steady-state volume of ghosts (○) and spherical intact red blood cells (□) as functions of temperature. The osmolalities used at each temperature were determined from Fig. 1 such that there were less than 10% ghosts in the intact cell suspensions, and more than 95% ghosts in the ghost suspensions.

select the best osmolality. These ghost-volume results are very different from those of the spherical, intact cells, in that they increase linearly with temperature, from 136 μm^3 at 0°C to 164 μm^3 at 40°C (a 21% increse in volume and a 13% increase in surface area).

Temperature and osmotic dependence of volume

Fig. 7 shows the osmotic dependence of sample modal volume, plotted against inverse osmolality, for cells stored at 0°C and 40°C. From the linear portions of the curves the R values of 0.62 ± 0.06 for 0°C, and 0.74 ± 0.06 for 40°C, are calculated *. As tabulated by Ponder [17], R values have been

* Ponder [17] analyzed data of this nature with the equation: $V = R \cdot W\ (1/\tau - 1) + V_0$, where τ is the relative tonicity, (mosmolal/300), W is the volume of the cell occupied by water at isotonicity, and V_0 is the isotonic volume.

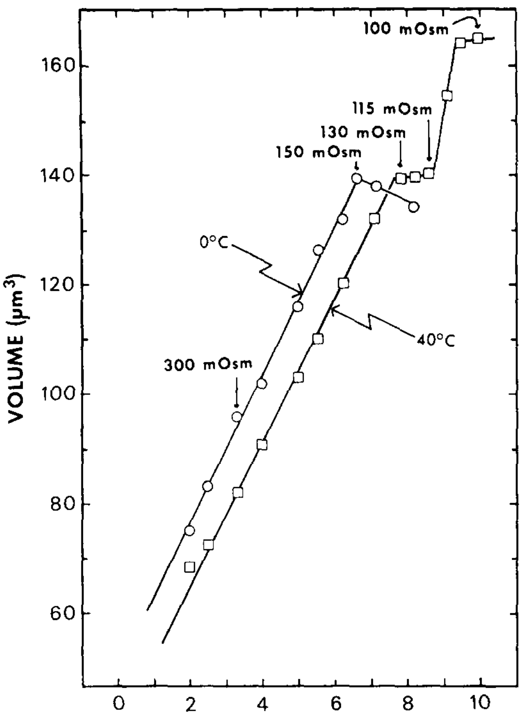

Fig. 7. The steady-state volume of red blood cells (i.e. mixtures of intact cells and, if sufficiently hypotonic, also ghosts) as a function of the inverse osmolality for solutions at 0°C (○) and 40°C (□). The percentage of intact red cells and ghosts at each osmolality is found by referencing Fig. 1.

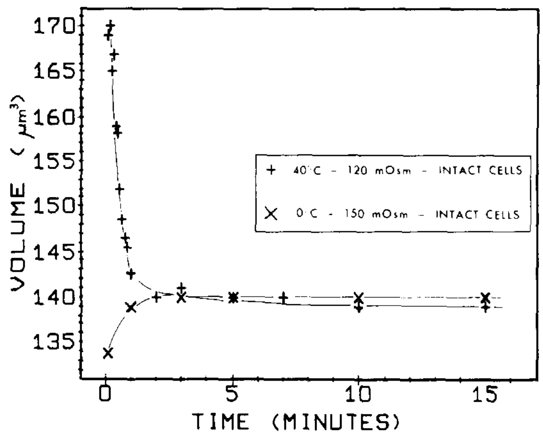

Fig. 8. Kinetics of volume change for red blood cells at 0°C and 40°C, after exposure to hypotonic solutions that result in less than 10% ghosts. (+, 120 mosmolal at 40°C; ×, 150 mosmolal at 0°C).

reported to be as low as 0.5 to as high as 0.95, depending on experimental conditions. The slopes of the curves of Fig. 7 are seen to be nearly identical, and equal to 300 $R \cdot W$ (mosmolal · μm^3). As the temperature is increased, the isotonic volume decreases, which decreases the amount of water in the cell (W), thus leading to a higher value for R. The temperature-independence of the slope of these curves has been previously reported [18].

From Fig. 7 we see that below 150 mosmolal, responses of the red cells to hypotonic media are markedly different for the two temperatures studied. In analyzing Fig. 7, it is important to emphasize that each volume is a modal cell volume for an entire (and in some cases mixed) population. As the cells hemolyze to a significant extent, the population shifts to an ever-increasing proportion of ghosts, as indicated by Fig. 1. Thus, at 0°C and 150 mosmolal (the point of maximum value for the 0°C curve), the percentage of ghosts is approx. 25%. Along with the increase to more than 95% ghosts, as the osmolality is further lowered, is an associated reduction in modal volume. At 40°C, the percentage of ghosts increases from 0% at the start of the first plateau (at 130 mosmolal), to 25% at the end of the plateau (115 mosmolal). Still-lower osmolalities result in an increase to more than 95% ghosts (by 100 mosmolal). In this case, however, there is an associated increase in the model volume until the size levels off at approx. 164 μm^3.

Kinetic effects. The volume-data of Fig. 7 represent steady-state values, where the cells were exposed to secondary dilutions of various osmolalities for at least 15 min. The time-dependent volume changes leading to some of these steady-state values were investigated as well, by transferring aliquots of red cells stored in isotonic solutions, at both 0°C and 40°C, to low-osmolality solutions, at temperatures matching the storage temperature. These osmolalities were chosen so as to lead to fewer than 10% ghosts for reasons similar to those stated above.

The kinetic results are given in Fig. 8. At 0°C, the low-osmolality solution induces rapid swelling to the cell's spherical volume, followed by a general leveling-off in volume. At 40°C the observations are much different. In the 120 mosmolal solution the cells swell up far beyond the steady-state spherical volume, but then quickly shrink back down to their steady state value. Note that the early-time maximum volume attained for the intact cells was even greater than 164 μm^3, which is the steady-state volume of ghosts made at this temperature (Fig. 6).

Discussion

In the Introduction, we presented five proposals to explain the temperature-dependence of osmotic fragility. One of these proposals will be considered only briefly, then discarded. Proposal 5, that the osmotic response of the cell is temperature-dependent, is refuted by the data of Fig. 7 (same slope for the intact cells at both 0°C and 40°C), as well as by the results of Dalmark [18].

The substance of Proposal 3 is a temperature-dependent increase in the potassum leak for the swollen cell. At first sight one might tend toward discarding this idea, relying on the data of Livne and Raz [9]: no difference in the pre-lytic potassum leak found. However, because of the manner in which they analyzed and plotted their data (as percent hemoglobin release vs. percent potassium release), and taking into consideration the recent finding that there is a temperature-dependent component to the amount of hemoglobin trapped within the cell following hemolysis [19], we are unable to completely discard proposal three.

Two other causes offered for the temperature dependence of osmotic fragility are (a) that the temperature influences the isotonic volume of the cell, our proposal (and model) 1, or (b) that changes in temperature alter the surface area of the cell at constant volume, our proposal (and model) 2.

In seeking an explanation for our measured changes in volume with changing temperature, we also introduced a third model of cell behavior, involving changes solely in shape factor, at constant volume and constant surface area. Large distortions in shape would be required to match the necessary (calculated) shape factors, which range from 1.12 to 1.31 (Table I). Since such changes are not seen in the microscope, nor have there been such reports in the literature, this model, will not be considered further. (Note: A pure change in shape, alone, should have no influence on fragility.)

Surface area and isotonic volume

Waugh and Evans [6] reported values for the temperature-dependence of red cell surface area, based on direct measurements using the micropipet method, coupled with certain assumptions about volume changes. They concluded that the red cell surface area increased fractionally by $1.2 \cdot 10^{-3}$/degree C, corresponding to a 4.8% increase from 0°C to 40°C.

Our measurements, in fact, show that over the temperature range of 0°C to 40°C the spherical intact cells must all have the same surface area since they all have the same volume, to within $\pm$ 1% (Fig. 6). This indicates that there must be a true temperature-dependent (isotonic) volume change, our Proposal 1, to account for the experimental data given in Table I.

The underlying cause of this temperature-dependence of isotonic volume is unknown. It is not likely caused by an in-leakage of sodium or an out-leakage of potassium ions since (a) the effect is rapidly reversible [4], and (b) it quickly reaches a steady state (Fig. 5). A possible explanation involves the temperature effect on the pK_a of hemoglobin. Increasing temperature is known to reduce the pH of a (normal hematocrit) red cell suspension in an unbuffered medium by 0.015 pH units/degree C [19]. The circumstance of inducing the cytoplasm to become, initially, more acidic than the medium is equivalent to placing the cell in a more basic, higher pH, medium, and this is known to cause the cell to lose water and shrink [20,21]. Thus, temperature-induced volume changes can be interpreted in terms of pH-induced volume changes, which are reversible (satisfies (a)), and fairly rapid (satisfies (b)) [21].

Osmotic fragility

From analysis of the data in Fig. 7, we can demonstrate that the volume change that occurs with increasing temperature (Fig. 3) is not, by itself, sufficient to cause the large reduction in fragility of the cells. That is, from Fig. 7, a 20 mosmolal difference is exactly balanced (to produce the same intact-cell volume) by the 40°C change; yet from Fig. 1 there is a 35 mosmolal difference between the osmolality for 50% hemolysis at 0°C and that at 40°C. Thus, another factor must be responsible for almost half of the decrease in osmotic fragility. An understanding of this new factor can be found in a close examination of Figs. 7 and 8.

At 0°C the cells swell at constant surface area until they become spheres, at 150 mosmolal with 25% ghosts (Figs. 1 and 7). As the osmolality is further decreased the cells continue to hemolyze and the model volume of the population actually decreases. At 40°C the cells also swell at constant surface area until they become spherical (at 130 mosmolal). Contrary to the behavior at 0°C, no ghosts are formed by the time this break-point in the curve is reached (Fig. 1). With a further decrease in osmolality to 115 mosmolal, no change appears to occur: a plateau has been reached where the cells do not increase further in size. Furthermore, by 115 mosmolal only about 25% of them have hemolyzed. With a further decrease in osmolality the modal volume of the mixed population increases markedly, along with an increase to over 95% ghosts. (This second steep-portion of the 40°C curve results from the dual population of the sample: intact spherical cells sizing at 140 μm^3 mixed with ghosts sizing at 164 μm^3.)

The transient behavior of the osmotically stressed cells (Fig. 8) underlies and results in the 130–115 mosmolal plateau for the 40°C curve. At 0°C the cells are seen to behave 'normally', swelling up to spheres (140 μm^3) without any increase in the spherical volume. That is, the 0°C curve does not rise above the initial spherical volume attained. However, at 40°C the cells exposed to 120 mosmolal are able, for short times, to swell far beyond the spherical volume of 140 μm^3 without undergoing hemolysis, but then (those able to resist hemolysis) quickly shrink back down to their steady-state volume. Since less than 10% actually hemolyze, the inescapable conclusion is that, at higher temperature, the intact cell membrane is able to expand greatly for a short period of time. (This essentially eliminates a role of any significance for our Proposal 4, an increase in membrane mechanical strength at constant volume and surface area, since we can now account for the full temperature dependence without it.)

To summarize, the transition from disk to sphere occurs at constant surface area [22,23], but contrary to widespread belief, the first spherical volume reached by a swelling red cell need not be equal to the cell's hemolytic volume. In contrast, the true hemolytic volume is temperature-dependent, increasing monotonically with increasing temperature.

The results given in Fig. 8 appear to be the first to clearly show that cells, subjected to abrupt osmotic stress, can undergo a very large transient stretch and still recover to their 140 μm^3 spherical volume. It should be noted that this conclusion stands in contrast to that drawn by other workers, using the micropipet method, namely that an increase of only 4% in the surface area will cause hemolysis [24].

Ghost volumes

The steady-state ghost volumes in Fig. 6 are seen to increase linearly with temperature and are presumed to be close to (yet below) the hemolytic volume. If the transient membrane expansion is greater than that corresponding to the hemolytic volume, the cell not only hemolyzes and subsequently reseals, but the cell membrane loses its elastic restoring capability, and remains permanently in an enlarged state. (From Fig. 7, 40°C compared to 0°C, this steady-state stretch in area is $(164/140)^{2/3}$ or 11%.) This behavior is consistent with the observations of others where deformations have been induced in other ways, such as by micropipet or mechanical elongation. When the red cell is deformed with a mild stress, which is then removed, the cell returns to its normal shape (elastic or viscoelastic behavior). But if a certain yield stress is exceeded, the deformation becomes irreversible (plastic behavior) [25,26].

Proposed mechanism for membrane extensibility

The underlying basis for the membrane's 'stretchability', within the bounds for mechanical integrity, is most likely the spectrin cytoskeletal network. This network, in its lowest energy state, probably exists in a folded, coiled, or otherwise not-fully-extended form. Evidence for such a 'globular' form for spectrin has been reported by Ralston [27], Branton [28], and used by Waugh [26] in his membrane modeling. (That the membrane can expand under other circumstances, when treated with anaesthetics, has been reported in other work [29].)

The high-temperature kinetic freedom of this coiled cytoskeletal network apparently allows the cell membrane to increase to a large size, without necessarily rupturing. If the cell does not hemolyze, the overall 'restoring' forces are evidently sufficient to restore the cytoskeleton-cell-membrane complex to its previous unstrained state. These restoring forces may include both a mechanical part (the extended spectrin returning to its coiled form), and an ionic part (a potassium leak, followed by water leakage, occurring to reduce the volume and the strain). (In support of this latter are the results of an additional experiment carried out in high-KCl medium to limit the potassium out-flow and thus to inhibit recovery. The hemolysis in such a case was increased from 23 to 49 percent, data not shown.)

References

1 Jacobs, M.H. and Parpart, A.K. (1931) Biol. Bull. 60, 95–119
2 Hoffman, J.F., Eden, M., Barr, J.S. and Bedell, R.H.S. (1958) J. Cell. Physiol. 51, 405–414
3 Seeman, P., Sauks, T., Argent, W. and Kwant, W.O. (1969) Biochim. Biophys. Acta 183, 476–489
4 Jacobs, M.H., Glassman, H.N. and Parpart, A.K. (1936) J. Cell. Comp. Physiol. 8, 403–417
5 Murphy, J.R. (1967) J. Lab. Clin. Med. 69, 758–775
6 Waugh, R. and Evans, E.A. (1979) Biophys. J. 26, 115–132
7 Ponder, E. and Robinson, E.J. (1934) Biochem. J. 28, 1940–1943
8 Davson, H. (1937) J. Cell. Comp. Physiol. 10, 247–264
9 Livne, A. and Raz, A. (1971) FEBS Lett. 16, 99–101
10 Aloni,, B., Eitan, A. and Livne, A. (1977) Biochim. Biophys. Acta 465, 46–53
11 Dulbecco, R. and Vogt, M. (1954) J. Exp. Med. 99, 167–199
12 Yee, J.P. and Mel, H.C. (1978) Biorheology 15, 321–339
13 Akeson, S.P. and Mel, H.C. (1982) Biochim. Biophys. Acta 718, 201–211
14 Gear, A.R.L. (1977) J. Lab. Clin. Med. 90, 914–928
15 Akeson, S.P. and Mel, H.C. (1983) Biophys. J. 44, 397–403
16 Grover, N.B., Naaman, J., Ben-Sasson, S. and Doljanski, F. (1969) Biophys. J. 9, 1398–1414
17 Ponder, E. (1971) in Hemolysis and Related Phenomena, pp. 50–114, Grune and Stratton, New York
18 Dalmark, M. (1975) J. Physiol. 250, 65–84
19 Jausel-Husken, S. and Deuticke, B. (1981) J. Membrane Biol. 63, 61–70
20 Hladky, S.B. and Rink, T.J. (1977) in Membrane Transport in Red Cells (Ellory, J.C. and Lew, V.T., eds.), pp. 115–135, Academic Press, New York
21 Jacobs, M.H. and Stewart, D.R. (1942) J. Gen. Physiol. 25, 539–552
22 Canham, P.B. and Parkinson, D.R. (1970) Can. J. Physiol. Pharm. 48, 369–376
23 Evans, E.A. and Leblond, P.F. (1973) Biorheology 10, 393–404
24 Evans, E.A., Waugh, R. and Melnik, L. (1976) Biophys. J. 16, 585–595
25 Evans, E.A. and Hochmuth, R.M. (1977) J. Membrane Biol. 30, 351–362
26 Waugh, R.E. (1982) Biophys. J. 39, 273–278
27 Ralston, G.B. (1976) Biochim. Biophys. Acta 455, 163–172
28 Branton, D. (1983) in The Harvey Lectures, Series 77, pp. 23–42, Academic Press, New York
29 Franks, N.P. and Lieb, W.R. (1981) Nature 292, 248–251